

Progress in radiomics of common heart disease based on cardiac magnetic resonance imaging

Jing-Le Fei¹, Cai-Ling Pu¹, Fang-Yi Xu¹, Yan Wu¹, Hong-Jie Hu^{1,*}

¹Department of Radiology, Sir Run Run Shaw Hospital, Zhejiang University School of Medicine, 310000 Hangzhou, P. R. China

*Correspondence: hongjiehu@zju.edu.cn (Hong-Jie Hu)

DOI:10.31083/j.jmcm.2021.01.801

This is an open access article under the CC BY 4.0 license (<https://creativecommons.org/licenses/by/4.0/>).

Submitted: 24 September 2020 Revised: 12 November 2020 Accepted: 04 February 2021 Published: 20 March 2021

As an innovative imaging processing mode, radiomics can extract microscopic information from images for quantitative analysis. The selected features and machine learning model can provide valuable data for clinical decisions in heart disease. Up till now, several studies have demonstrated the role of radiomics in the accurate diagnosis and discrimination of heart disease as well as in the prognosis assessment of the patient with heart disease. Cardiac Magnetic Resonance (CMR) displays a wide range of advantages, such as multi-parameter, multi-sequence, multi-plane, and no radiation. CMR has advantages in noninvasive assessment of structural and functional heart disease. This paper reviews the workflow and related studies on common heart disease based on CMR images in radiomics.

Keywords

Radiomics; Myocardial infarction; Hypertrophic cardiomyopathy; Dilated cardiomyopathy; Myocarditis; Cardiac magnetic resonance

1. Content

Radiomics is an emerging field for image analysis. It can extract many invisible features by high-throughput computing and convert them into exploitable high-dimensional data. The research subject of radiomics can be any pictures, and the research process is orderly and controllable. Different steps are required to reach that aim: image collection, image segmentation, feature extraction, and modeling. The identified features based on the histogram as first order feature, followed by shape feature, texture features and high order features can be combined in clinic application and provide disease diagnosis, adverse event prediction, survival analysis, and prognosis assessment [1]. Over the years, radiomics has attracted scholars worldwide. Because radiomics analysis can acquire a lot of microscopic information, and it also can be carried out simultaneously with other clinical procedures, improving ipso facto the health care system by shortening the study time of images by radiologists.

At present, radiomics has been successfully used in tumors: considering lung cancer studies by extracting features from ground glass nodules resulting in a confident classification of diseases [2, 3]; also involved in the studies of hepatocellular carcinoma (HCC) with promising advances in the evaluation of hepatic diseases, determining immunologic index, treatment and prognostication [4–6]. Lately, it has been

illustrated that microvascular invasion (MVI) represented an independent factor for early recurrence and poor prognosis of HCC [7, 8]. Many reports have covered that the models with MVI imaging characteristics were superior to the single clinical index model [9, 10]. Those successful applications in tumors are the starting point to an extension of radiomics to cardiac disease studies. Though in early years, echocardiography based on radiomics was used to differentiate diseases, such as amyloidosis [11]. Due to the poor repeatability of echocardiography, the relevant research failed to make a breakthrough. Therefore, the application of radiomics in heart disease may need to be based on other examination methods.

CMR is a no-radiation examination and can offer images with multi-parameter, multi-sequence, and multi-plane. So it becomes one of the most critical methods for noninvasive assessment of structural and functional heart disease. For instance, cine sequence is useful for evaluating the cardiac function, and the late gadolinium enhancement (LGE) sequence helps to determine the existence of myocardial fibrosis. The first pass perfusion can assess myocardial filling defect, while the T2 weighted sequence detects the formation of myocardial edema. CMR assists in the diagnosis and evaluates the prognosis of heart disease. It has been shown in some studies that HCM patients with delayed enhancement on LGE sequence had a 3.4-fold increased risk of sudden cardiac death and a 1.8-fold increase in all-cause mortality [12]. It was reported that delayed enhancement on the LGE sequence may be a potential matrix for ventricular arrhythmia in the DCM population [13]. Kunze *et al.* [14] reported that in patients with revascularization after myocardial infarction, the natural T1 signal value was correlated with peripheral monocyte count ($P = 0.024$); so T1 signal value was related to systemic inflammatory activity.

Recently, scholars have developed a strong interest in radiomics based on CMR images (Table 1). Their studies have achieved good results in myocardial infarction (MI), hypertrophic cardiomyopathy (HCM), dilated cardiomyopathy (DCM), and myocarditis. Therefore, the aim of this paper is to review the workflow and related studies on common heart disease based on CMR images in radiomics.

Table 1. Selected studies using radiomics for the diagnosis of common heart disease.

Heart disease	Year	Publication	Image substrate	Sample size	Important feature	Performance
Myocardial infarction	2018	Gibbs <i>et al.</i> [38]	LGE	76	Kurtosis and skewness	AUC = 0.73
	2019	Androulakis <i>et al.</i> [24]	LGE	154	Entropy	HR = 3.20
	2018	Baessler <i>et al.</i> [27]	Cine	180	Teta1, Perc.01, Var-iance, WavEnHH.s-3, and S(5,5) SumEntrp	AUC = 0.93
Hypertrophic	2019	Neisius <i>et al.</i> [18]	T1 mapping	232	Run-length non-enrichment [RLN]-135°, [SRHGE]-135°, LBP-15, LBP-20, LBP-25, and LBP-28	AUC = 0.89
Cardiomyopathy (Myocardial hypertrophy)	2018	Schofield <i>et al.</i> [42]	Cine	216	mean value, standard deviation, entropy, kurtosis, average positive pixel, and skewness	AUC = 0.89
	2018	Amano <i>et al.</i> [44]	LGE	23	entropy LL	AUC = 0.72
	2018	Cheng <i>et al.</i> [45]	LGE	67	X0_GLRLM_energy, X0_H_skewness and X0_GLCM_cluster_tendency	HR = 0.78
	2020	Alis <i>et al.</i> [30]	LGE	64	GlcM_V1_Sum_Varc, GlcM_N3Di_Varc, GlcM_V1_Sum_Of_Sqs, GlcM_V5_Sum_Averg, GrIm_VG_Lev_Non_Un, GlcM_V5_Ang_Sc_Mom, and Gab8H4Mag	AUC = 0.92
	2018	Baebler <i>et al.</i> [17]	T1-weighted	62	GLenNonU, WavEnLL, and Fraction	AUC = 0.95
	2020	Neisius <i>et al.</i> [47]	T1 mapping/LGE	217	LRLGE-45°, LBP-22, LBP-16, homogeneity-4, and LBP-1	C-index = 0.75
Dilated cardiomyopathy	2018	Shao <i>et al.</i> [49]	T1 mapping	74	P10, P25, P50, P75, P90, Mode, SD, Maximum, Mean, homogeneity, entropy and contrast	Accuracy = 0.85
	2019	Muthalaly <i>et al.</i> [51]	LGE	130	entropy	HR = 3.5
Myocarditis	2018	Baessler <i>et al.</i> [37]	T1 and T2 mapping	39	T2-rluni, T2 sum entropy, and T2-GLenNonU	AUC = 0.88
	2019	Baessler <i>et al.</i> [58]	T1 and T2 mapping	31	average T2 time and T2-GLNU	AUC = 0.76

LGE, late gadolinium enhancement; AUC, Area Under Curve; HR, hazard ratio; Local binary patterns; LBP (The gray value of the center pixel is taken as the threshold, and the corresponding binary code is obtained to represent the local texture feature); X0 features (They are extracted from the original image).

2. Workflow of radiomics

The primary process of radiomics is meant to draw the region of interest (ROIs), obtain a large number of features, and then filter the data to receive robust and informative optimal features. Finally, model training and testing are carried out (Fig. 1). The specific steps are designed as follows:

2.1 Image acquisition and preprocessing

Images acquired during traditional CMR (including short and long axis, T1/T2 weighted, initial perfusion pass, and late gadolinium enhancing sequences) are selected for radiomics analysis. Recent studies tend to preferentially select late gadolinium enhancement and cine sequences images [15, 16], while the use of the remaining sequences is gradually increasing [17, 18]. Image preprocessing methods include image resampling and data normalization. Image resampling is to change the image voxel resolution to 1 mm³ and the image size to 256³ voxels. It is used to eliminate the influence of the heterogeneity of MRI scanner models (such as image resolution, slice thickness, and patient position) [19]. Data standardization refers to unifying the indicators of different dimensional units into the same order of magnitude, eliminating the influence of different dimensional units on the results. For example, the original image maximum pixel matrix

value is 256, and 1 is the minimum; after processing, the image value is comprised between an interval of 0-1 [20].

2.2 Image segmentation

Image segmentation is used to outline ROIs on images for further feature selection and model building, and segmentation methods could be divided into three types consisting of manual, semi-automatic, and fully automatic segmentation algorithms [21]. Manual segmentation is time-costing but could promise accurate and reliable outcomes. The automatic algorithm could reduce the contour work for doctors dramatically with high operation repeatability. However, the automatic segmentation algorithm is not as popularized as the manual algorithm, and the accuracy of automatic segmentation is still to be improved. In CMR, the endocardium and epicardium of the left ventricle and endocardium of the right ventricle are often delineated on short-axis images, which define the boundaries of the left ventricular myocardium and the two ventricular blood pools. After the selection of ROIs, data can be extracted; data changes as ROIs change. Therefore, most studies are carried out based on the automatize selection and manually adjusting of ROIs, with better chances of repeatability [21] (Fig. 2).

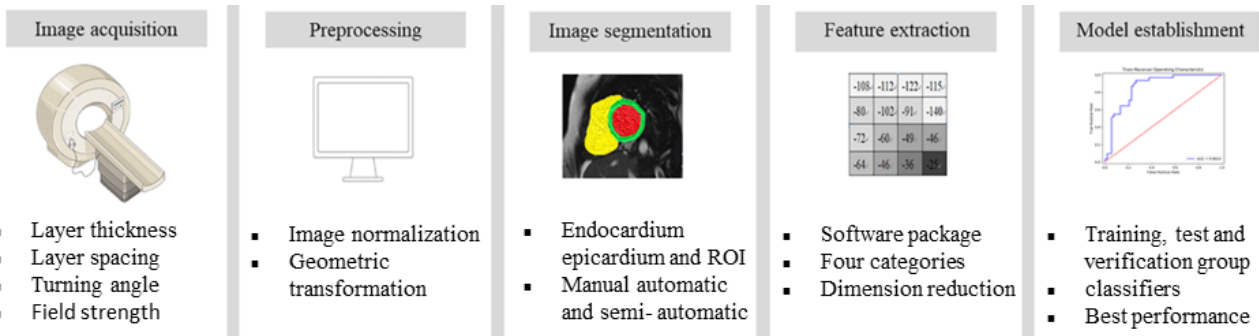


Fig. 1. The basic process of radiomics and the factors influence the results.

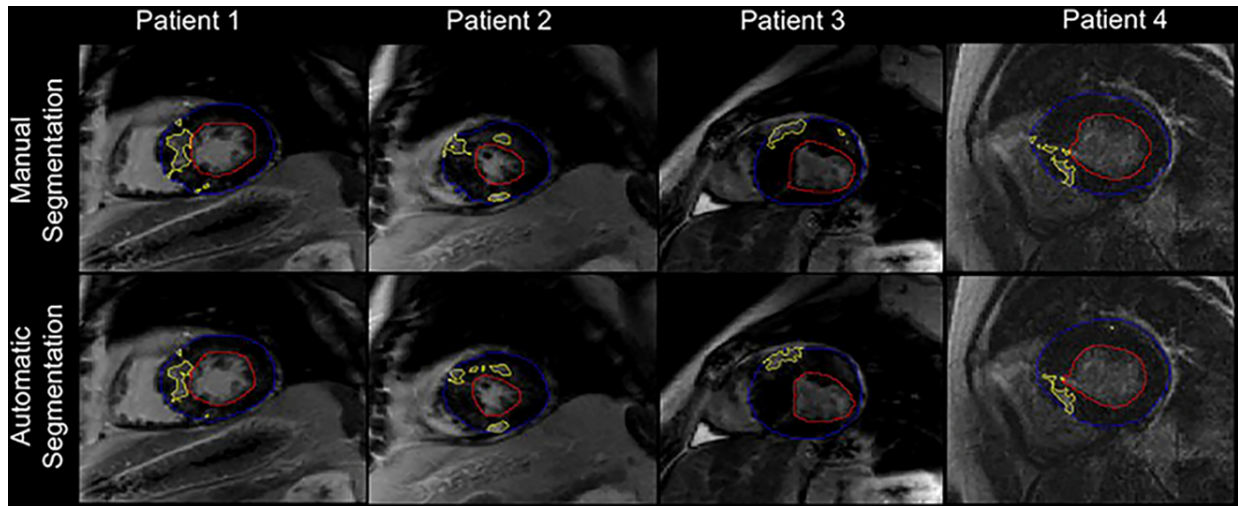


Fig. 2. On LGE images, we obtained the segmentation results of scar and myocardium of four different patients. The epicardial boundary was blue, the endocardial boundary was red and the scar was yellow. There were two segmentation methods: manual segmentation (previous line) and automatic segmentation (next row). Automatic image segmentation had better repeatability. Cited in [22].

2.3 Feature extraction and selection

Feature extraction is a crucial step for radiomics research. Routine images are converted into plenty of quantitative data. It is these quantitative features that combine image information with clinical practice. Radiomics features represent the geometry of ROIs, the distribution and the spatial correlation of signal strength of voxels in ROIs. These features can be divided into four categories:

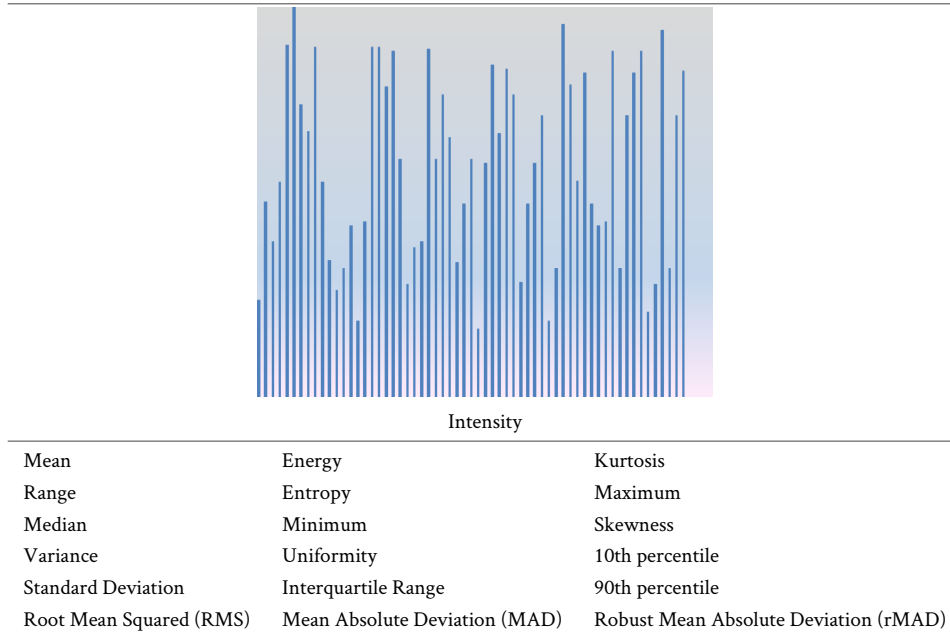
a) first order features: derived from the ventricular contour to define voxel intensity distribution in ROIs (the principle is shown later), such as energy, kurtosis, skewness, and entropy (Table 2). In 1948, Shannon *et al.* [23] initially proposed that entropy could describe the quantitative information relative to the communication system. In CMR protocol, entropy is used to evaluate the heterogeneity of pixel signal strength composed by a mixture of fibrotic tissue and normal myocardium. Based on this application, many studies have reported the implication of entropy in the diagnosis and prognosis of common heart disease [24].

b) shape features: determining the size and shape of ROIs in two or three dimensions. They include not only the conventional features like length, volume, and the sur-

face of ROIs, but also features describing the overall shape of ROIs, such as compactness, sphericity, and elongation (Table 3). Shape features are independent of the gray intensity of the image, so they are only acquired through the original image [25].

c) texture features: describing the distribution and the interaction of voxels in ROIs and using digital quantization eigenvalues to describe the image information (Table 4). Quantitative texture features can be relatively objective parameters for diagnosis or prognosis prediction in the clinic, compared with conventional qualitative judgment based on a medical picture. The first step of texture feature analysis is to build the signal strength matrix. Each voxel within the ROIs is assigned to a value accordingly to the different intensity, and then a signal strength form is constructed to form a signal strength matrix. Next, we can directly calculate the signal histogram of the signal strength matrix, which forms the first order features mentioned above. However, the first order features represent the overall signal distribution within ROIs. More complex algorithms are needed to describe the correlation between each adjacent voxel. Through the complex calculation and reconstruction of the original signal strength

Table 2. According to the signal strength matrix, the first order features based on histogram can be constructed by simple arithmetic model. The abscissa is the intensity value of voxel signal, and the ordinate is the frequency of occurrence. The statistical data obtained from the histogram are summarized, and the specific first order features are listed.



matrix, a new matrix can be formed, such as gray level co-occurrence matrix (GLCM), gray level run length matrix (GLRLM), and gray level size zone matrix (GLSZM). GLCM is basically constructed according to the frequency of different signal strength pairs in the original signal strength matrix. Corresponding measures such as contrast (local variation) and entropy (confusion) can then be calculated; these features reflect the gray level changes of signal strength pairs and the degree of confusion in ROIs [26]. GLRLM is constructed by the number of consecutive runs along the specified direction in the signal strength matrix. It can evaluate the spatial correlation of any number of voxels (not just pairs). For example, run entropy reflects the degree of confusion in the gray distribution of the stroke length (higher value is more chaotic); high gray level run emphasis measures the distribution of higher gray values (higher value results in a greater concentration of higher gray values). GLSZM is reconstructed by quantifying the number of voxels within the same signal strength in the image, such as gray level non uniformity and gray level variance. Many scholars have confirmed the value of Gray level non uniformity (GLN) in the diagnosis and differential diagnosis of myocarditis [27].

d) high order feature: filter or high order image parameters are added to first order or texture features, such as Wavelet, Laplace of Gaussian, and autoregressive model. There may be redundant features or features not closely related to the results [28].

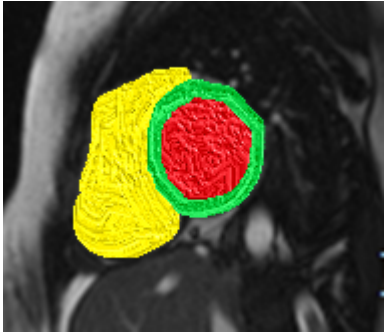
The number of extracted features can reach thousands. So feature selection (such as principal component analysis or clustering) will identify and delete redundant and unstable image features [29]. It will avoid the overfitting of the model.

2.4 Modeling and validation

The purpose of radiomics is to develop a model for diagnosis, prognosis, and treatment evaluation of medical diseases. A radiomics model is developed using specific classifiers for model training. There are kinds of classifiers, including random forest (RF), support vector machine (SVM), naive Bayes, and k-nearest neighbor method (K-NN) [30]. RF is composed of many decision trees; each decision tree comprises random samples and random features. The final judgment will be made through the summary of all the decision trees' results [31]. Its advantage is that there will be no overfitting phenomenon if there are enough decision trees, while too many trees will slow down the algorithm speed. SVM uses a separation hyperplane to partition the training set correctly. It can tolerate some wrong samples in the boundaries, thus improving the robustness and generalization of the model [32]. Naive Bayes is based on probability theory and assumes that each feature is independent and suitable for small sample classification. The principle of K-NN is to take the k training samples nearest to the test samples. The category with the most frequent occurrence in these k samples is the classification result. The disadvantage of K-NN is that it has higher requirements for the balance of sample categories.

All these classifiers can be used for modeling, but the classifier which shows the best performance is preferable. Training sets, verification sets and testing sets are very important in the process of radiomics analysis. Generally, the data is distributed into several groups: training sets used to fit the model, and verification sets used to adjust parameters of the model but also for preliminary evaluation of the model, while

Table 3. The left and right ventricular blood pools (red, yellow) and left ventricular myocardium (green) are segmented. The shape features of radiomics can be deduced from the contour of left and right ventricle, and the specific shape features can be listed.

	2D	3D
	Mesh Surface	Mesh Volume
	Pixel Surface	Voxel Volume
	Perimeter	Surface Area
	Perimeter to Surface ratio	Surface Area to Volume ratio
	Sphericity	Sphericity
	Spherical Disproportion	Compactness
	Maximum 2D diameter	Spherical Disproportion
	Major Axis Length	Maximum 3D diameter
	Minor Axis Length	Major Axis Length
	Elongation	Minor Axis Length
		Least Axis Length
		Elongation
		Flatness

the testing sets used to evaluate the final generalization effect of the model. For instance, K-NN was used to identify whether HCM patients occur ventricular arrhythmia (the Area Under Curve (AUC) = 0.92), but the research lacked testing sets. Hence, it was impossible to evaluate the generalization effect of the model, and further research was needed [30]. The model is representative only if the sample size is large enough; experts propose k-fold cross-validation for the defect that there are insufficient clinical research samples [33]. The training sets are split into k samples, and one of them is randomly selected as the verification sample, and the remaining k-1 is the training sample. The process is repeated k times to obtain the best performance. Usually, k is acceptable for sampling when its value is between 5 and 10. If k is less than 5, the underfitting problem could occur [34].

3. Progress of radiomics applying to heart disease

3.1 Application of radiomics in myocardial infarction

MI is one of the most serious cardiovascular diseases threatening human health, and the main pathophysiological mechanism is myocardial ischemia and necrosis due to coronary artery stenosis and occlusion [35]. Patients have the risk of ventricular arrhythmia and poor left ventricular remodeling [36]. Baessler *et al.* [37] studied the efficacy of texture features in diagnosing subacute and chronic myocardial infarction on CMR cine images. The results showed that the five texture features Teta1, Perc.01, Variance, Wavenhh.s-3, and S (5,5) SumEntrp had statistical significance in differentiating infarcted myocardium from normal myocardium. In the multiple Logistic regression models, diagnostic accuracy of MI was excellent (AUC = 0.93). Gibbs *et al.* [38] explored the relationship between the features based on the Laplacian of a Gaussian filter and scar heterogeneity and arrhythmia events. The results showed that the kurtosis ($P=0.005$) and skewness ($P=0.046$) of MI patients with arrhythmia events were significantly higher than those without arrhythmia events. An-

droulakis *et al.* [24] used the entropy based on CMR-LGE images to measure scar heterogeneity parameters in patients with myocardial infarction and the entire left ventricular myocardium. In the multivariate analysis results, the risk of ventricular arrhythmia increased by 1.9-fold for every unit of entropy increase in scar tissue (hazard ratio: 1.9; 95% confidence interval: 1.0-3.5; $P = 0.042$), indicating that entropy may be related to the fibrous scar causing the arrhythmia. For each unit increase in entropy throughout the left ventricle, the risk of death increased 3.2 times (hazard ratio: 3.2; 95% confidence interval: 1.1-9.9; $P = 0.038$), suggesting that the entropy of the entire left ventricle may reflect the fibrosis pattern associated with poor cardiac remodeling. However, there was no statistically significant difference in the patient's entropy with or without ventricular arrhythmia ($P = 0.07$) in this study. Some scholars analyzed that it may be due to the loss of the spatial relationship between pixels and original pixels when the intensity signal value was input. So entropy could not be directly applied to image data analysis [39].

3.2 Application of radiomics in hypertrophic cardiomyopathy

HCM is the most common primary cardiomyopathy, with a prevalence of around 1/500. The diagnostic criteria for HCM are end-diastolic left ventricular wall thickness ≥ 15 mm, or the patient with a family history of HCM in whose end-diastolic left ventricular wall thickness ≥ 13 mm and excluding hypertensive cardiomyopathy, valvular heart disease, and other cardiac diseases secondary to ventricular wall thickening [40]. Among the patients with genetically positive HCM, 23% had hypertension simultaneously [41], so the differential diagnosis of HCM and hypertensive heart disease is particularly important in clinical diagnosis and treatment. Neisius *et al.* [18] analyzed the texture of the images with native scanning T1-mapping and showed that these six features, namely, Run-length non-enrichment [RLN]-135°, [SRHGE]-135°, LBP-15, LBP-20, LBP-25, and LBP-28, can differentiate HCM and hypertensive heart disease, with the

Table 4. Texture features describe the relationship of signal strength distribution between adjacent voxels. It is a new signal strength matrix reconstructed by different arithmetic methods according to the original signal strength matrix.

Texture Features									
Gray Level Co-occurrence Matrix (GLCM)	Level	Gray Level Size Zone Matrix (GLSZM)	Matrix	Gray Level Run Length Matrix (GLRLM)	Matrix	Gray Level Dependence Matrix (GLDM)	Matrix	Neighbouring Tone Difference Matrix (NGTDM)	Gray
Autocorrelation		Emphasis		Run Emphasis		Small Dependence Emphasis (SDE)		Coarseness	
Average		Gray Level Non-Uniformity (GLN)		Gray Level Non-Uniformity (GLN)		Large Dependence Emphasis (LDE)		Contrast	
Cluster		Gray Level Non-Uniformity Normalized (GLNN)		Gray Level Non-Uniformity Normalized (GLNN)		Gray Level Non-Uniformity (GLN)		Busyness	
Contrast		Size-Zone Non-Uniformity (SZN)		Run Length Non-Uniformity (RLN)		Dependence Non-Uniformity (DN)		Complexity	
Entropy		Zone Percentage (ZP)		Run Length Non-Uniformity Normalized (RLNN)		Dependence Non-Uniformity Normalized (DNN)		Strength	
Variance		Gray Level Variance (GLV)		Run Percentage (RP)		Gray Level Variance (GLV)			
Energy		Zone Variance (ZV)		Gray Level Variance (GLV)		Dependence Variance (DV)			
Informational Measure of Correlation (IMC)		Zone Entropy (ZE)		Run Variance (RV)		Dependence Entropy (DE)			
Inverse Difference Moment (IDM)	Difference Moment	Low Gray Level Zone Emphasis (LGLZE)		Run Entropy (RE)		Low Gray Level Emphasis (LGLE)			
Maximal Correlation Coefficient (MCC)	Correlation Coefficient	High Gray Level Zone Emphasis (HGLZE)		Low Gray Level Run Emphasis (LGLRE)		High Gray Level Emphasis (HGLE)			
Maximum Probability		Small Area Low Gray Level Emphasis (SALGLE)		High Gray Level Run Emphasis (HGLRE)		Small Dependence Low Gray Level Emphasis (SDLGLE)			
Sum of Squares		Small Area High Gray Level Emphasis (SAHGLE)		Short Run Low Gray Level Emphasis (SRLGLE)		Small Dependence High Gray Level Emphasis (SDHGLE)			
		Large Area Low Gray Level Emphasis (LALGLE)		Short Run High Gray Level Emphasis (SRHGLE)		Large Dependence Low Gray Level Emphasis (LDLGLE)			
		Large Area High Gray Level Emphasis (LAHGLE)		Long Run Low Gray Level Emphasis (LRLGLE)		Large Dependence High Gray Level Emphasis (LDHGLE)			
				Long Run High Gray Level Emphasis (LRHGLE)					

maximum diagnostic accuracy of 86.2%. Schofield *et al.* [42] tried to use these six first order features of the cine images to distinguish left ventricular hypertrophy causes on the unenhanced cine sequence images, which were mean value, standard deviation, entropy, kurtosis, average positive pixel, and skewness. The results showed that compared with the normal control group, HCM and non-compaction of the ventricular myocardium had the best performance, and the six texture features had significant statistical significance ($P < 0.001$). In aortic stenosis disease, except entropy, the remaining five texture features had significant statistical significance ($P < 0.001$). In hypertensive heart disease, except for skewness, the remaining five texture features were statistically significant. In the differential diagnosis of disease, these six texture features were statistically significant in the differential diagnosis of non-compaction of the ventricular myocardium and aortic stenosis, and the better result

appeared between hypertrophic cardiomyopathy and aortic stenosis disease (AUC = 0.89). These studies demonstrated that radiomics could assist clinicians in the differential diagnosis of HCM and other diseases that cause left ventricular hypertrophy.

Most patients with HCM have a good prognosis, but a small number of patients have adverse cardiac events, such as adverse cardiac remodeling, malignant arrhythmia, sudden cardiac death. Some scholars believe that a key mechanism of adverse events is myocardial fibrosis. Since Choudhury *et al.* [43] first reported the evaluation of HCM fibrosis by delayed enhancement of LGE sequence in 2002, more and more studies have confirmed that the existence and degree of delayed enhancement were related to the occurrence of adverse cardiac events. In recent years, many studies have begun to explore the relationship between CMR-LGE texture features and cardiac adverse events. As far as we know,

Amano *et al.* [44] reported, for the first time, the correlation between CMR-LGE image texture features of HCM and ventricular arrhythmia. The results showed that among the four texture features, the entropy LL of patients with arrhythmia was significantly smaller than that of patients without arrhythmia ($P = 0.0058$), the area under the curve of entropy LL was 0.72, and the area under the curve of delayed enhancement was 0.96. Although entropy LL was weaker than delayed enhancement in distinguishing HCM from ventricular tachycardia in this study, entropy LL was indeed a discriminating factor for HCM with or without ventricular tachycardia. Unlike previous scholars, Cheng *et al.* [45] magnified the focus from several specific texture features to 90 features extracted from images and studied the correlation between LGE-CMR texture features and poor prognosis of HCM patients with systolic dysfunction. The results showed that the higher X0_GLRLM_energy, lower X0_H_skewness and lower X0_GLCM_cluster_tendency were positively correlated with adverse events ($P < 0.05$), suggesting that increased myocardial heterogeneity was associated with adverse cardiac events in HCM patients. Alis *et al.* [30] proposed whether texture analysis based on CMR-LGE image can identify ventricular arrhythmia in HCM patients. The results showed that ventricular arrhythmias in HCM can be identified using a K-NN classifier with 94% diagnostic accuracy (AUC = 0.92). This study's highlight is not limited to a few texture features, but also through the method of radiomics to screen features and establish a model to evaluate the correlation between radiomics and cardiac adverse events. However, due to the small sample size, the research trains and verifies all the data without external testing, so it is impossible to evaluate generalization efficiency.

HCM is usually found in youth, so some patients need to have multiple CMR examinations during long-term follow-up. Gadolinium-based contrast agents are the most common contrast mediums used in CMR examination. However, gadolinium is a contraindication for patients with renal failure, and it will cause nephrogenic systemic fibrosis. This is because after receiving gadolinium-based contrast agents in patients with renal function impairment, the clearance rate of contrast medium in vivo is slowed down, and Gd^{3+} is more easily released from the chelate, which promotes the production of chemokines and growth factors by macrophages and monocytes; it can also stimulate the production of hyaluronic acid, fibronectin, and types I and III collagens. Therefore, patients with impaired renal function are prone to nephrogenic systemic fibrosis [46]. Accordingly, Baebler *et al.* [17] used texture analysis on T1 weighted images of HCM patients without contrast to identify the differences between HCM and normal myocardium. Results showed that the four texture features were gray level non-uniformity ($P < 0.001$), energy of wavelet coefficients in low frequency sub-bands ($P < 0.001$), fraction ($P < 0.001$) and sum average ($P = 0.007$), which provided a new parameter for the evaluation of HCM by contrast free T1 weighted images. Neisius *et al.* [47]

used texture analysis on T1 mapping images of HCM patients to identify a delayed enhancement on LGE sequences. The results showed that the five texture features, LRLGE-45°, LBP-22, LBP-16, homogeneity-4, and LBP-1, had the greatest contribution value to the DTE classifier. In the DTE classifier, the c-index of the training set was 0.75, and that of the test set was 0.74. The learning DTE classifier could identify some LGE negative patients, suggesting that about 1/3 of LGE negative patients could avoid using gadolinium-based contrast agents, consistent with nearly 50% of HCM patients without delayed enhancement in previous studies [48], that may contribute unnecessarily to the use of contrast media in the future. The above studies show that radiomics plays an important role in diagnosing, differential diagnosis, and prognosis evaluation of HCM, which provides a new technology and direction for future HCM research.

3.3 Application of radiomics in dilated cardiomyopathy

The etiology of DCM can be either primary or secondary. This disease is characterized by left ventricular or right ventricular dilatation with contractile dysfunction. The diagnosis of DCM remains a major clinical challenge because of the exclusion of ischemic cardiomyopathy and other non-ischemic cardiomyopathies that may produce a pattern similar to the left ventricular remodeling. Shao *et al.* [49] studied whether texture analysis on the T1-mapping image of SVM was helpful to DCM diagnosis. The results showed that the SVM classifier's diagnostic accuracy based on a meaningful histogram of the T1-mapping MRI image and GLCM was 85%. This method may provide an auxiliary tool for objective quantitative evaluation of clinical DCM diagnosis. Accurate risk stratification of sudden cardiac death is essential for the prognosis of patients with DCM.

The accuracy of left ventricular ejection fraction (LVEF) used to be a risk stratification index is limited and is greatly affected by the operator. Therefore, scholars hope to explore a new parameter to assist the risk stratification assessment of DCM. Myocardial fibrosis in patients with DCM provides a material basis for ventricular arrhythmia [50]. Myocardial heterogeneity is formed by the coexistence of different types and degrees of fibrous tissue with viable myocardium. Muthalaly *et al.* [51] used radiomics methods and hypothesized that the left ventricular myocardium heterogeneity was considerable in DCM patients requiring primary prevention by CMR assessment; that is, the entropy value was enormous, and the risk of ventricular arrhythmia was also greater. It showed that when judging whether DCM patients had an arrhythmia, left ventricular entropy was statistically significant in univariate factor analysis and multivariate factor analysis ($P < 0.05$), suggesting that entropy was an independent predictor of ventricular arrhythmia in DCM patients risk factors. After 2.4 years of follow-up, no arrhythmia occurred in patients with LVEF $< 35\%$ and left ventricular entropy < 4.46 , indicating that left ventricular entropy can provide a stable and straightforward risk assessment method for DCM patients. At present, the incidence rate of radiomics studies

in DCM is still low, probably because the DCM diagnosis is not clear enough, the incidence of DCM is low, and the DCM wall is thin, and it is not easy to draw ROIs.

3.4 The application of radiomics in myocarditis

The viral infection is the most common cause of myocarditis, with an incidence rate of 20/10000 and a mortality rate of 4.8/100000 [52, 53]. The disease pathological changes comprise myocardial edema, degeneration, necrosis, and lymphocyte infiltration [54, 55]. Myocarditis is asymptomatic in mild cases, but severe arrhythmia, acute cardiac insufficiency, and sudden cardiac death have been noticed in some cases. The “gold standard” for diagnosing myocarditis is the endomyocardial biopsy, but the examination is invasive and has low sensitivity, so it is not widely used in clinical practice [56, 57]. CMR provides specific value for non-invasive diagnosis of myocarditis. Noninvasive diagnosis of myocarditis is still one of the challenging problems in clinical practice. Baessler *et al.* [27] analyzed the T1 and T2 mapping images of patients with acute infarct myocarditis similar to acute infarct myocarditis using radiomics. They found that these three texture features were statistically different between patients with positive and negative endocardial biopsy ($P < 0.05$), which were T2-rluni, T2 sum entropy, and T2-GLevNonU. In the classification model composed of two run-length matrix features (T2-rluni and T2-GLevNonU), the AUC was 0.88, so these two features could well diagnose patients with acute infarct myocarditis. Besides, Baessler *et al.* [58] evaluated the diagnostic value of imaging radiomics parameters for myocarditis in heart failure patients. They found that the combination of the two features of average T2 time and T2-GLNU had the highest diagnostic performance in patients with acute heart failure myocarditis (AUC = 0.76, 95% confidence interval: 0.43-0.95), the combination of T2_kurtosis and T1-GLevNonU in myocarditis patients with chronic heart failure had the highest diagnostic performance (AUC = 0.85, 95% confidence interval: 0.57-0.90). In patients with acute and chronic heart failure with myocarditis, the difference in texture features with the best performance may reflect the two diseases different pathological changes. In the diagnosis of myocarditis, the texture features based on T2 images perform well, mainly because myocarditis is closely related to myocardial edema. So the T2 sequence maybe the best choice to observe myocardial water content of CMR. In summary, it has particular potential research value in the diagnosis and differential diagnosis of myocarditis.

4. Summary of radiomics of cardiomyopathies

In summary, radiomics based on CMR has made certain research progress in common heart disease such as MI, HCM, DCM, and myocarditis. However, it is traditional parameters that are still used as references in clinical decision-making, not radiomics. So the application value of radiomics is still not well defined. We may need to solve the following prob-

lems: Firstly, CMR scan time is long, and the time resolution is not as good as ultrasound; CMR is not suitable for some special populations, such as claustrophobia and elderly and frail patients. Secondly, it is difficult to obtain enough heart disease in a single-center, suggesting that radiomics research may require multicenter cooperation to study heart disease. Finally, for the sake of repeatability and comparability of radiomics research, it is essential to use standardized imaging protocols. However, radiomics is still in the embryonic stage and mainly focuses on texture features in the study of heart disease. At present, studies on feature extraction, feature selection and classifier training of heart disease are not enough. Therefore, to achieve better clinical decision-making, we should overcome these challenges and perform further studies to prove the role of radiomics in heart disease.

Author contributions

Design and initial draft: Jing-Le Fei.

Critical Review and revisions: Cai-Ling Pu, Fang-Yi Xu, Yan Wu, Hong-Jie Hu.

Final approval of manuscript: Jing-Le Fei, Cai-Ling Pu, Fang-Yi Xu, Yan Wu, Hong-Jie Hu.

Acknowledgment

Thanks a lot for Umba Mabombo Pierre’s English support.

Funding

National Natural Science Foundation of China (NSFC) under Grant No. 81873908.

Conflict of interest

The authors declare no conflicts of interest statement.

References

- [1] Lambin P, Leijenaar RTH, Deist TM, Peerlings J, de Jong EEC, van Timmeren J, *et al.* Radiomics: the bridge between medical imaging and personalized medicine. *Nature Reviews Clinical Oncology*. 2017; 14: 749-762.
- [2] Hofmanninger J, Langs G. Mapping visual features to semantic profiles for retrieval in medical imaging. *Proceedings of the IEEE Conference on Computer Vision and Pattern Recognition (CVPR)*. 2015; 457-465.
- [3] Yang Y, Yang Y, Zhou X, Song X, Liu M, He W, *et al.* EGFR L858R mutation is associated with lung adenocarcinoma patients with dominant ground-glass opacity. *Lung Cancer*. 2015; 87: 272-277.
- [4] Kloth C, Thaiss WM, Kärger R, Grimmer R, Fritz J, Ioanoviciu SD, *et al.* Evaluation of texture analysis parameter for response prediction in patients with hepatocellular carcinoma undergoing drug-eluting bead transarterial chemoembolization (DEB-TACE) using biphasic contrast-enhanced CT image data. *Academic Radiology*. 2017; 24: 1352-1363.
- [5] Kuo MD, Gollub J, Sirlin CB, Ooi C, Chen X. Radiogenomic analysis to identify imaging phenotypes associated with drug response gene expression programs in hepatocellular carcinoma. *Journal of Vascular and Interventional Radiology*. 2007; 18: 821-830.
- [6] Oh J, Lee JM, Park J, Joo I, Yoon JH, Lee DH, *et al.* Hepatocellular carcinoma: texture analysis of preoperative computed tomography images can provide markers of tumor grade and disease-free survival. *Korean Journal of Radiology*. 2019; 20: 569.

- [7] Lim K, Chow PK, Allen JC, Chia G, Lim M, Cheow P, *et al.* Microvascular invasion is a better predictor of tumor recurrence and overall survival following surgical resection for hepatocellular carcinoma compared to the Milan criteria. *Annals of Surgery*. 2011; 254: 108-113.
- [8] Mazzaferro V, Llovet JM, Miceli R, Bhoori S, Schiavo M, Mariani L, *et al.* Predicting survival after liver transplantation in patients with hepatocellular carcinoma beyond the Milan criteria: a retrospective, exploratory analysis. *The Lancet Oncology*. 2009; 10: 35-43.
- [9] Peng J, Zhang J, Zhang Q, Xu Y, Zhou J, Liu L. A radiomics nomogram for preoperative prediction of microvascular invasion risk in hepatitis B virus-related hepatocellular carcinoma. *Diagnostic and Interventional Radiology*. 2018; 24: 121-127.
- [10] Zhu YJ, Feng B, Wang S, Wang LM, Wu JF, Ma XH, *et al.* Model-based three-dimensional texture analysis of contrast-enhanced magnetic resonance imaging as a potential tool for preoperative prediction of microvascular invasion in hepatocellular carcinoma. *Oncology Letters*. 2019; 18: 720-732.
- [11] Pinamonti B, Picano E, Ferdeghini EM, Lattanzi F, Slavich G, Landini L, *et al.* Quantitative texture analysis in two-dimensional echocardiography: application to the diagnosis of myocardial amyloidosis. *Journal of the American College of Cardiology*. 1989; 14: 666-671.
- [12] Weng Z, Yao J, Chan RH, He J, Yang X, Zhou Y, *et al.* Prognostic value of LGE-CMR in HCM. *JACC: Cardiovascular Imaging*. 2016; 9: 1392-1402.
- [13] Gulati A, Jabbour A, Ismail TF, Guha K, Khwaja J, Raza S, *et al.* Association of fibrosis with mortality and sudden cardiac death in patients with nonischemic dilated cardiomyopathy. *Journal of the American Medical Association*. 2013; 309: 896.
- [14] Kunze KP, Dirschinger RJ, Kossmann H, Hanus F, Ibrahim T, Laugwitz K, *et al.* Quantitative cardiovascular magnetic resonance: extracellular volume, native T1 and 18F-FDG PET/CMR imaging in patients after revascularized myocardial infarction and association with markers of myocardial damage and systemic inflammation. *Journal of Cardiovascular Magnetic Resonance*. 2018; 20: 33.
- [15] Balaban G, Halliday BP, Bai W, Porter B, Malvuccio C, Lamata P, *et al.* Scar shape analysis and simulated electrical instabilities in a non-ischemic dilated cardiomyopathy patient cohort. *PLoS Computational Biology*. 2019; 15: e1007421.
- [16] Gould J, Porter B, Claridge S, Chen Z, Sieniewicz BJ, Sidhu BS, *et al.* Mean entropy predicts implantable cardioverter-defibrillator therapy using cardiac magnetic resonance texture analysis of scar heterogeneity. *Heart Rhythm*. 2019; 16: 1242-1250.
- [17] Baeßler B, Mannil M, Maintz D, Alkadhi H, Manka R. Texture analysis and machine learning of non-contrast T1-weighted MR images in patients with hypertrophic cardiomyopathy-Preliminary results. *European Journal of Radiology*. 2018; 102: 61-67.
- [18] Neisius U, El-Rewaify H, Nakamori S, Rodriguez J, Manning WJ, Nezafat R. Radiomic analysis of myocardial native T1 imaging discriminates between hypertensive heart disease and hypertrophic cardiomyopathy. *JACC: Cardiovascular Imaging*. 2019; 12: 1946-1954.
- [19] Chaddad A, Kucharczyk MJ, Daniel P, Sabri S, Jean-Claude BJ, Niazi T, *et al.* Radiomics in glioblastoma: current status and challenges facing clinical implementation. *Frontiers in Oncology*. 2019; 9: 374.
- [20] Eagle. The purpose and function of normalization [EB/OL]. 2017. <https://blog.csdn.net/zenghaitao0128/article/details/78361038> (Accessed: 15 July 2020).
- [21] Hassani C, Saremi F, Varghese BA, Duddalwar V. Myocardial radiomics in cardiac MRI. *American Journal of Roentgenology*. 2020; 214: 536-545.
- [22] Leiner T, Rueckert D, Suiesiaputra A, Baeßler B, Nezafat R, Išgum I, *et al.* Machine learning in cardiovascular magnetic resonance: basic concepts and applications. *Journal of Cardiovascular Magnetic Resonance*. 2019; 21: 61.
- [23] Shannon CE. A mathematical theory of communication. *Bell System Technical Journal*. 1948; 27: 379-423.
- [24] Androulakis AFA, Zeppenfeld K, Paiman EHM, Piers SRD, Wijngaalen AP, Siebelink HJ, *et al.* Entropy as a novel measure of myocardial tissue heterogeneity for prediction of ventricular arrhythmias and mortality in post-infarct patients. *JACC: Clinical Electrophysiology*. 2019; 5: 480-489.
- [25] Lorensen WE, Cline HE. Marching cubes: a high resolution 3D surface construction algorithm. *ACM SIGGRAPH Computer Graphics*. 1987; 21: 163-169.
- [26] Haralick RM, Shanmugam K, Dinstein I. Textural features for image classification. *IEEE Transactions on Systems, Man, and Cybernetics*. 1973; SMC-3: 610-621.
- [27] Baessler B, Luecke C, Lurz J, Klingel K, von Roeder M, de Waha S, *et al.* Cardiac MRI texture analysis of T1 and T2 maps in patients with infarctlike acute myocarditis. *Radiology*. 2018; 289: 357-365.
- [28] Avanzo M, Stancanello J, El Naqa I. Beyond imaging: the promise of radiomics. *Physica Medica*. 2017; 38: 122-139.
- [29] Raisi-Estabragh Z, Izquierdo C, Campello VM, Martin-Isla C, Jaggi A, Harvey NC, *et al.* Cardiac magnetic resonance radiomics: basic principles and clinical perspectives. *European Heart Journal-Cardiovascular Imaging*. 2020; 21: 349-356.
- [30] Alis D, Guler A, Yergin M, Asmakutlu O. Assessment of ventricular tachyarrhythmia in patients with hypertrophic cardiomyopathy with machine learning-based texture analysis of late gadolinium enhancement cardiac MRI. *Diagnostic and Interventional Imaging*. 2020; 101: 137-146.
- [31] Yang D, Rao G, Martinez J, Veeraraghavan A, Rao A. Evaluation of tumor-derived MRI-texture features for discrimination of molecular subtypes and prediction of 12-month survival status in glioblastoma. *Medical Physics*. 2015; 42: 6725-6735.
- [32] Chen S, Zhou S, Yin F, Marks LB, Das SK. Investigation of the support vector machine algorithm to predict lung radiation-induced pneumonitis. *Medical Physics*. 2007; 34: 3808-3814.
- [33] Krstajic D, Buturovic LJ, Leahy DE, Thomas S. Cross-validation pitfalls when selecting and assessing regression and classification models. *Journal of Cheminformatics*. 2014; 6: 10.
- [34] Jung Y. Multiple predicting K-fold cross-validation for model selection. *Journal of Nonparametric Statistics*. 2018; 30: 197-215.
- [35] Thygesen K, Alpert JS, White HD. Universal definition of myocardial infarction. *Journal of the American College of Cardiology*. 2007; 50: 2173-2195.
- [36] Schelbert EB, Piehler KM, Zareba KM, Moon JC, Ugander M, Messroghli DR, *et al.* Myocardial fibrosis quantified by extracellular volume is associated with subsequent hospitalization for heart failure, death, or both across the spectrum of ejection fraction and heart failure stage. *Journal of the American Heart Association*. 2015; 4: e002613.
- [37] Baessler B, Mannil M, Oebel S, Maintz D, Alkadhi H, Manka R. Subacute and chronic left ventricular myocardial scar: accuracy of texture analysis on nonenhanced cine MR images. *Radiology*. 2018; 286: 103-112.
- [38] Gibbs T, Villa ADM, Sammut E, Jeyabraba S, Carr-White G, Ismail TF, *et al.* Quantitative assessment of myocardial scar heterogeneity using cardiovascular magnetic resonance texture analysis to risk stratify patients post-myocardial infarction. *Clinical Radiology*. 2018; 73: 1059.e17-1059.e26.
- [39] Tandri H, Okada DR. Ventricular arrhythmias in ischemic cardiomyopathy. *JACC: Clinical Electrophysiology*. 2019; 5: 490-492.
- [40] Elliott P, Andersson B, Arbustini E, Bilinska Z, Cecchi F, Charron P, *et al.* Classification of the cardiomyopathies: a position statement from the European society of cardiology working group on myocardial and pericardial diseases. *European Heart Journal*. 2007; 29: 270-276.
- [41] Gruner C, Ivanov J, Care M, Williams L, Moravsky G, Yang H, *et al.* Toronto hypertrophic cardiomyopathy genotype score for prediction of a positive genotype in hypertrophic cardiomyopathy. *Circulation Cardiovascular Genetics*. 2013; 6: 19-26.
- [42] Schofield R, Ganeshan B, Fontana M, Nasis A, Castelletti S, Ros-

- mini S, *et al.* Texture analysis of cardiovascular magnetic resonance cine images differentiates aetiologies of left ventricular hypertrophy. *Clinical Radiology*. 2019; 74: 140-149.
- [43] Choudhury L, Mahrholdt H, Wagner A, Choi KM, Elliott MD, Klocke FJ, *et al.* Myocardial scarring in asymptomatic or mildly symptomatic patients with hypertrophic cardiomyopathy. *Journal of the American College of Cardiology*. 2002; 40: 2156-2164.
- [44] Amano Y, Suzuki Y, Yanagisawa F, Omori Y, Matsumoto N. Relationship between extension or texture features of late gadolinium enhancement and ventricular tachyarrhythmias in hypertrophic cardiomyopathy. *BioMed Research International*. 2018; 2018: 4092469.
- [45] Cheng S, Fang M, Cui C, Chen X, Yin G, Prasad SK, *et al.* LGE-CMR-derived texture features reflect poor prognosis in hypertrophic cardiomyopathy patients with systolic dysfunction: preliminary results. *European Radiology*. 2018; 28: 4615-4624.
- [46] Todd DJ, Kay J. Gadolinium-induced fibrosis. *Annual Review of Medicine*. 2016; 67: 273-291.
- [47] Neisius U, El-Rewaidy H, Kucukseymen S, Tsao CW, Mancio J, Nakamori S, *et al.* Texture signatures of native myocardial T1 as novel imaging markers for identification of hypertrophic cardiomyopathy patients without scar. *Journal of Magnetic Resonance Imaging*. 2020; 52: 906-919.
- [48] Chan RH, Maron BJ, Olivotto I, Pencina MJ, Assenza GE, Haas T, *et al.* Prognostic value of quantitative contrast-enhanced cardiovascular magnetic resonance for the evaluation of sudden death risk in patients with hypertrophic cardiomyopathy. *Circulation*. 2014; 130: 484-495.
- [49] Shao X, Sun Y, Xiao K, Zhang Y, Zhang W, Kou Z, *et al.* Texture analysis of magnetic resonance T1 mapping with dilated cardiomyopathy. *Medicine*. 2018; 97: e12246.
- [50] Iles L, Pfluger H, Lefkovits L, Butler J, Kistler M, Kaye M, *et al.* Myocardial fibrosis predicts appropriate device therapy in patients with implantable cardioverter-defibrillators for primary prevention of sudden cardiac death. *Journal of the American College of Cardiology*. 2011; 57:821-828.
- [51] Muthalaly RG, Kwong RY, John RM, van der Geest RJ, Tao Q, Schaeffer B, *et al.* Left ventricular entropy is a novel predictor of arrhythmic events in patients with dilated cardiomyopathy receiving defibrillators for primary prevention. *JACC: Cardiovascular Imaging*. 2019; 12: 1177-1184.
- [52] Heymans S, Eriksson U, Lehtonen J, Cooper LT. The quest for new approaches in myocarditis and inflammatory cardiomyopathy. *Journal of the American College of Cardiology*. 2016; 68: 2348-2364.
- [53] Pollack A, Kontorovich AR, Fuster V, Dec GW. Viral myocarditis-diagnosis, treatment options, and current controversies. *Nature Reviews Cardiology*. 2015; 12: 670-680.
- [54] Biesbroek PS, Beek AM, Germans T, Niessen HWM, van Rossum AC. Diagnosis of myocarditis: current state and future perspectives. *International Journal of Cardiology*. 2015; 191: 211-219.
- [55] García-Becerril GE, Cruz-Montalvo AE, De La Cruz MA, Ares MA, Moreno-Ruiz LA, García-Chequer AJ, Maldonado-Bernal C, *et al.* Differential expression of coxsackievirus and adenovirus receptor in endomyocardial tissue of patients with myocarditis. *Molecular Medicine Reports*. 2019; 20: 2189-2198.
- [56] Blagova O, Osipova Y, Nedostup A, Kogan E, Zaitsev A, Fomin V. Diagnostic value of different noninvasive criteria of latent myocarditis in comparison with myocardial biopsy. *Cardiology*. 2019; 142: 167-174.
- [57] Nakayama T, Murai S, Ohte N. Dilated cardiomyopathy with eosinophilic granulomatosis with polyangiitis in which active myocardial inflammation was only detected by endomyocardial biopsy. *Internal Medicine*. 2018; 57: 2675-2679.
- [58] Baessler B, Luecke C, Lurz J, Klingel K, Das A, von Roeder M, *et al.* Cardiac MRI and texture analysis of myocardial T1 and T2 maps in myocarditis with acute versus chronic symptoms of heart failure. *Radiology*. 2019; 292: 608-617.